Computing and Visualization in Science manuscript No.
(will be inserted by the editor)

Blood flow through compliant vessels after endovascular repair: wall deformations induced by the discontinuous wall properties

Sunčica Čanić *

Department of Mathematics, University of Houston, Houston TX 77204-3476, USA
(http://www.math.uh.edu/~canic)

The date of receipt and acceptance will be inserted by the editor

Abstract. In this paper we derive a set of equations which can be used to study wall deformations and transmural pressure at the anchoring sites of endovascular prostheses. The equations are the jump conditions associated with the underlying model equations. The model equations are derived from the Navier-Stokes equations to describe the blood flow through compliant axi-symmetric vessels after endovascular repair. They are in the form of a quasilinear hyperbolic system of partial differential equations with discontinuous coefficients. Since the weak form of the equations contains the product of the Dirac delta distribution with the Heaviside function, the jump conditions and the weak form cannot be obtained using the standard distribution theory. Driven by the undelying application in mind, we present a preliminary analysis leading to the jump conditions by interpreting the ambiguous products as a mean value with respect to the measure obtained in the limit of the "regularizing kernels" [17]. We show that the numerical solution obtained by using the Richtmyer two-step Lax-Wendroff method satisfies the weak form of the equations associated with a symmetric regularizing kernel in which case the weak form is independent of the particular choice of the kernel. We give an example (treatement of aortic abdominal aneurysm using multiple overlapping stents) where the conditions obtained in this paper can be used in the optimal design of an endovascular procedure.

1 Introduction

Endovascular prostheses are used in the treatment of various cardiovascular diseases (aneurysm, vascular lesions, stenosis, occlusions) to either replace or repair failing blood vessels. Endovascular prostheses vary from non-destensible (Dacron) tubes to elastic metal coils called stents. After every cardiovascular surgery or endovascular repair during which an endovascular prosthesis has been inserted in the aorta, the wall properties of the compliant vessel change in the region where the prosthesis is placed. Measurements [5] indicate that, for example, stiffness of Bare-Metal Wallstents which are used in the treatment of abdominal aneurysm to replace the aneurysmal part of the abdominal aorta, is ten times smaller than the typical stiffness of the native abdominal aorta. Furthermore, in cases when endovascular stents are used to keep the vessel from closure by supporting the wall of a failing artery, it has been reported that arterial walls change their elastic properties after deployment of endovascular stents by "loosing their expansive properties"[1] and becoming less compliant.

In this paper we study the effects of the rapidly changing elastic wall properties on the wall deformations and on the blood flow. We consider a one-dimensional model of blood flow through an axisymmetric compliant vessel whose elastic properties change abruptly in the axial direction, x, due to an inserted endovascular prosthesis. The model equations are in the form of a one-dimensional hyperbolic system of balance laws

$$\frac{\partial A}{\partial t} + \frac{\partial m}{\partial x} = 0, \tag{1}$$

$$\frac{\partial m}{\partial t} + \frac{\partial}{\partial x}\left(\frac{\alpha m^2}{A}\right) + \frac{1}{\rho} A \frac{\partial p}{\partial x} = f(A,m), \tag{2}$$

where $A(x,t)$ is the cross-sectional area of the vessel, $m(x,t) = AV$ is the momentum, $V = V(x,t)$ is the average axial velocity and p is the transmural pressure, which will be specified below. The coefficient α accounts for the fact that *averaged* quantities (momentum) are conserved; it is constant for a given velocity profile.

The source term $f = f_\nu + f_{\text{kink}}$ includes the effects of viscosity ν via

$$f_\nu(A,m) = -\frac{2\nu\alpha}{\alpha - 1} m/A$$

and, if the abdominal aorta is curved [3], the effects of the curvature $\kappa(x)$ via

$$f_{\text{kink}}(x,m) = -mB(x)\kappa(x)$$

* Research of the author is partly supported by the National Science Foundation under Grant DMS-9977372, by the University of Houston NSF REU supplement, and by the University of Houston TLCC grant.

where $B(x)$ is the 'fudge factor' which depends on the channel.

Versions of this model have been used by many authors to model fluid flow in compliant tubes ([2,8,9,14, 11]). In this paper, as in our earlier paper [3], we will assume that the transmural pressure is inhomogeneous

$$p(x,A) = G_0(x)\left[\left(\frac{A}{A_0}\right)^{\beta(x)/2} - 1\right] \qquad (3)$$

and that the coefficients that describe elastic properties of the vessel $G_0(x)$ and $\beta(x)$ are piecewise constant with jump discontinuities at the anchoring sites of the prosthesis. Here G_0 describes tissue stiffness (pressure-strain elastic modulus), and β describes linear/nonlinear behavior of the tube wall (pressure-strain relationship).

When G_0 and β are constant, system (1), (2) can be written in conservation form. It is well known that nonlinear hyperbolic conservation laws typically produce shock wave solutions even when the coefficients and the data are smooth. Of course, physiologically, a true shock in arterial circulation is not possible since blood viscosity and elasticity of the vessel wall preclude shock formation. However, it might be possible to generate very steep pressure gradients in the aorta, which are believed to correspond to the pistol-shut phenomenon, a loud cracking sound heard through a stethoscope placed at the radial or femoral artery, occurring in patients with aortic insufficiency. Under normal physiological conditions no such waves develop. Indeed, it was shown in [4] that under normal physiological conditions system (1), (2) does not produce shock wave solutions. The basic assumptions that guarantee smooth flow are the amplitude and frequency of pulsatile flow which need to fall in the "normal" regime, and the value of the elasticity parameters G_0 and β which need to correspond to a healthy individual [4].

In this paper we study properties of the solutions and potential problems with numerical simulations when the pressure coefficients (G_0 and β in this example) are discontinuous (piecewise constant). In that case the system can no longer be written in conservation form and the meaning of the weak form of the hyperbolic equations is ambiguous.

Even for hyperbolic systems of conservation laws with discontinuous coefficients, the literature is sparse. There are various difficulties associated with the solutions of such systems. For example, physically reasonable solutions exhibit jump discontinuities that are not compressive because the jump discontinuity in the solution is induced by the discontinuity in the coefficients, and not by the compressive structure of the characteristics. Deriving the "correct" entropy criterion for such jump discontinuities, and capturing such solutions numerically may be a problem. In the case when the equations are not in conservation form, as in the case of our model, verifying whether a numerical method captures correct weak solutions is nontrivial since the meaning of the weak form of the equations in unclear. In the case when the equations are linear and in conservation form there is a very nice theory developed in [10] that deals with numerical approximation of one-dimensional linear conservation equations with discontinuous coefficients. To the best of my knowledge there is no such theory available for the quasilinear hyperbolic problems with discontinuous coefficients.

In addition to the presence of noncompressive jump discontinuities, solutions of hyperbolic equations with discontinuous coefficients can develop WEAK FRONTS [6] at the points where the coefficients are discontinuous. Weak fronts are the waves across which only the first derivative in the solution has a jump discontinuity, but the solution itself stays continuous. Examples showing that both types of solutions arise in conservation laws with discontinuous coefficients will be presented in Section 2.

Regarding the behavior of the solutions of equations (1) and (2) we prove that at the points of discontinuity of the coefficients, the solution exhibits jump discontinuity in the cross-sectional area A and is continuous in the momentum m. Of course, a jump in the cross-sectional area should be regarded as a high gradient wall deformation in the physiological setting. Smoothing of the discontinuous coefficients in the model equations (1) and (2) would produce a smoothed wall profile. However, to estimate the size of the deformation and the corresponding transmural pressure, jump conditions can be used. To calculate the jump in A at the points where the coefficients are discontinuous weak form of the equations needs to be defined. Since equation (2) contains the product of the Dirac measure with the Heaviside function, which cannot be defined in the sense of distributions, new ideas need to be developed. Based on the results presented in [17] we define a weak solution which depends on the 'physics' of the problem through the regularization of the Dirac delta term by an 'admissible averaging kernel'. In the case when the kernel is symmetric, the weak solution is independent of the choice of the kernel. We show that the Richtmyer two-step Lax-Wendroff method [13] recovers the weak solution corresponding to the symmetric kernel. The reasons for this are under investigation by the author.

We use the Richtmyer two-step Lax-Wendroff method [13] to simulate equations (1) and (2) in the scenario corresponding to endovascular repair of abdominal aneurysm. The corresponding problem and data are specified in Section 5. The measurements of the stent properties are obtained by collaborator Dr. Ravi Chandar [5]. We investigate the use of multiple overlapping stents to bridge the aneurysmal cavity of the abdominal aorta. This problem was suggested by cardiologist Dr. Krajcer at St. Lukes' Hospital in Houston who uses multiple overlapping stents in his procedures. We suggest that the jump conditions obtained from the limiting weak form provide a tool to study optimal strategies in the treatment of aneurysm using multiple overlapping stents. This is because these equations provide information regarding transmural pressure and wall deformation at the anchoring sites of the stent. High transmural pressure and high deformations can be directly linked to various long and short term complications reported after endovascular repair of aortic aneurysm [16].

This paper is organized as follows. In Section 2 we present three simple scalar examples which show three different effects discontinuous coefficients can have on the analysis and properties of solutions of hyperbolic equations. The third example produces in nature the same qualitative behavior and exhibits the same difficulties associated with the formulation of the weak form of the equation as do the model equations (1) and (2). We develop the main ideas and theory here, and apply them to solve the problem in Example 3. In Section 3 we discuss numerical simulations of Example 3 and conclude that the Richtmyer two-step Lax-Wendroff method produces the weak solution obtained using a symmetric kernel in the weak formulation of the problem in Example 3. In Section 4 we apply the ideas developed in Section 2 to the equations (1) and (2). In this section we prove that A has a jump discontinuity but m is continuous at the points where the pressure coefficients jump; we also derive the weak form here and obtain the jump conditions across the locus where the coefficients are discontinuous. In Section 5 we show a numerical simulation obtained using the Richtmyer two-step Lax-Wendroff method to simulate the flow and wall deformations in the case when three overlapping stents are used in the repair of aortic abdominal aneurysm. We show that the wall deformations predicted by the jump conditions associated with a symmetric kernel are exhibited in the numerical simulation.

2 Motivating Examples

We motivate the results of this paper by three simple examples. The first example shows that quasilinear hyperbolic equations with discontinuous coefficients can have solutions that are continuous. At the points where the coefficients are discontinuous such solutions typically posses a discontinuity in the first derivative (weak fronts). The second example shows that conservation laws with spatially discontinuous coefficients can lead to the solutions that have a stationary jump discontinuity. Such discontinuities are typically not compressive. Furthermore, at the point x_* where the coefficients are discontinuous, new nonstationary waves (rarefaction or compressive shock waves) are generated. The weak form of the equations can be easily derived because the equation is in conservation form. Finally, the third example exhibits the main difficulty associated with solving quasilinear hyperbolic equations that are not in conservation form, and whose coefficients are discontinuous; namely, the difficulty that the weak form of the equations contains a nonconservative product of the Dirac delta function with the Heaviside function. We present our findings related to this problem in Example 3 and use the same approach to deal with equations (1) and (2) in the second half of this paper.

EXAMPLE 1. Consider the following quasilinear (Burgers') equation

$$u_t + a(x)uu_x = 0 \tag{4}$$

with the initial data

$$u_0(x) = \begin{cases} 0, & x < 0 \\ 1, & x > 0. \end{cases} \tag{5}$$

Suppose that the coefficient $a(x)$ is piecewise constant, with a jump discontinuity at $x = 1$

$$a(x) = \begin{cases} 1, & x < 1 \\ 2, & x > 1. \end{cases}$$

The characteristics of the equation are $\frac{dx}{dt} = a(x)u$, and the solution u is constant along the characteristics. A sketch of the solution is shown in Figure 1 . The solution and the characteristics have a kink at $x = 1$ where a is discontinuous.

Continuity of u is consistent with the weak formulation. Indeed, if we write equation (4) in conservation form

$$u_t + \left(\frac{1}{2}a(x)u^2\right)_x = \frac{1}{2}a'(x)u^2,$$

multiply by a test function $\phi \in C_0^\infty$ with compact support in a neighborhood D of the potential shock locus $x = x(t)$ in the (x,t)-plane, and integrate by parts, we obtain

$$\int\int_D \left(u\phi_t + \frac{1}{2}a(x)u^2\phi_x\right) = \int\int_D \frac{1}{2}a(x)\left(u^2\phi\right)_x.$$

If u is continuous, all the integrals are well defined and one obtains that across a shock traveling with speed s the following holds

$$-s[u] + \frac{1}{2}\left[au^2\right] = \frac{1}{2}\left[au^2\right],$$

where $[\cdot]$ denotes the jump in the corresponding quantities. This is consistent with the assumption that $[u] = 0$.

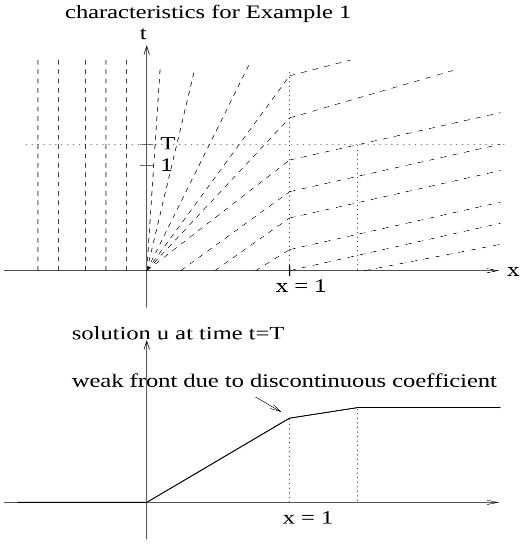

Fig. 1. Solution corresponding to Example 1

EXAMPLE 2. Consider the conservation law

$$u_t + \left(\frac{1}{2}a(x)u^2\right)_x = 0, \tag{6}$$

with $u_0(x) = 1$. Let a be a piecewise constant function given by

$$a(x) = \begin{cases} a_L, \; x < x_* \\ a_R, \; x > x_*. \end{cases} \tag{7}$$

Proposition 2.1. *The solution u cannot be continuous at x_*.*

Proof. Suppose that u is continuous at x_*. Weak formulation of the conservation law implies

$$-s\,[u] + \frac{1}{2}\left[au^2\right] = 0.$$

If u is continuous at x_*, we get $(a_R - a_L)u(x_*, t) = 0$, and so $a_L = a_R$ which is in contradiction with the assumption that a has a jump at x_*.

The jump in u can be calculated from the weak form and we present the solution below. At the points where a is discontinuous, the discontinuity in u is stationary, $s = 0$, and the weak form implies

$$a_R u_R^2 - a_L u_L^2 = 0, \quad \text{or} \quad u_R = \pm\sqrt{\frac{a_L}{a_R}} u_L.$$

The quasilinear from of the equations is

$$u_t + a(x)uu_x = -a'(x)u^2, \tag{8}$$

the characteristics are given by $\frac{dx}{dt} = a(x)u$. The solution u is constant along the characteristics everywhere except at x_* where it jumps by the amount calculated from the weak form of the equation. We will use this to present solutions in the following two cases

CASE 1: $a_L = 1$ and $a_R = 2$, $x_* = 1$. From the jump condition we calculate that $u_R = \sqrt{2}/2$ and the slope of the characteristics emanating from (x_*, t) becomes $\frac{dx}{dt} = \sqrt{2}$. The slope of the characteristics emanating from $(x, 0), x > x_*$ is given by $\frac{dx}{dt} = 2$. Since there is a gap in the wedge region bounded by the chracteristics emanating from $(x_*, 0)$ with the left slope $\frac{dx}{dt} = \sqrt{2}$ and the right slope $\frac{dx}{dt} = 2$ we can complete the solution by using the (entropy) rarefaction wave solution. See Figure 2 on the left.

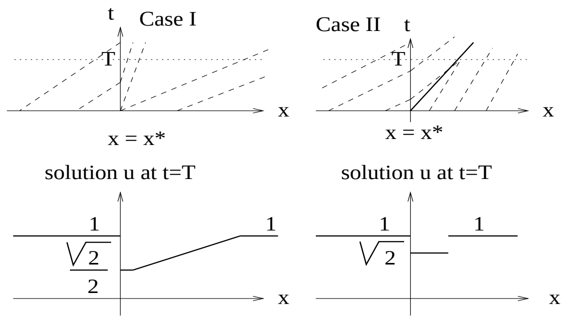

Fig. 2. Solutions corresponding to Example 2; Case 1 and Case 2.

CASE 2: $a_L = 2$ and $a_R = 1$, $x_* = 1$. In this case the jump condition implies that $u_R = \sqrt{2}$ and the slope of the characteristics emanating from x_* is $\frac{dx}{dt} = \sqrt{2}$. The characteristics emanating from $(x, 0)$ with $x > x_*$ have the slope $\frac{dx}{dt} = 1$, and so the data $u = 1$ travels slower than u_R. The solution must contain a shock between $u = u_R$ and $u = 1$ which propagates from $x = x_*$ with the speed given by

$$s = \frac{\left[\frac{1}{2}a(x)u\right]}{[u]} = \overline{u} = \frac{1}{2}(1 + \sqrt{2}),$$

where $\overline{u}$ is the average of the states located on either side of the shock (the shock speed for the classical Burgers' equation). A sketch of the solution is shown in Figure 2 on the right.

Notice that in this example new nonstationary wave are generated at $(x_*, 0)$.

EXAMPLE 3. Consider the following quasilinear hyperbolic equation

$$u_t + u\,(a(x)u)_x = 0 \tag{9}$$

with the initial data $u_0(x) = u_0$. Let a be a piecewise constant function given by (7).

Proposition 2.2. *If u is continuous and u_x bounded then u cannot be a solution of equation (9) when a is given by (7).*

Proof. Let D be a bounded subset of the (x, t)-plane such that $x = x_*$ passes through D. Multiplication of equation (9) by the test function $\phi \in C_0^\infty$ and integration by parts lead to

$$\int_D u_x\,(a(x)u)\,\phi + \int_D u\phi_t + au^2\phi_x = 0.$$

We can now proceed in the standard fashion by dividing these integrals in two, one over the subset D_1 and the other over the subset D_2, lying on either side of $x = x_*$ to obtain

$$\int_{D_1} u\phi_t + (au^2)\phi_x + u_x(au)\phi$$
$$+ \int_{D_2} u\phi_t + (au^2)\phi_x + u_x(au)\phi = 0.$$

Integration by parts and the divergence theorem lead to the following weak form that holds across the line $x = x_*$

$$\int_{x=x_*} \left([u]\,dx - \left[au^2\right] dt\right)\phi = 0 \quad \forall \phi \in C_0^1.$$

Therefore $\left[au^2\right] = 0$, which implies, since u is assumed continuous, that $a_L = a_R$. This is in contradiction with the assumption that a is discontinuous.

Proposition 2.2 implies that u cannot be continuous at x_* hense the weak form of the equation

$$\int u\phi_t + (au^2)\phi_x + \int u_x a(x)u\phi = 0 \tag{10}$$

is ambiguous because it contains the product $\int u_x a(x)u\phi$ of the Dirac delta distribution with the Heaviside function which cannot be defined in the sense of distributions.

We shall use the approach presented in [17] to treat these products as the mean value of the bounded measurable function with respect to the measure obtained in the limit of the regularizing kernels.

We introduce the *mean value with respect to x* of a bounded, measurable function v. Let $\psi(x,t)$ be a bounded, measurable function satisfying the conditions

$$\psi(x,t) \geq 0, \quad \psi(x,t) = 0 \quad \text{for} \quad |x| \geq 1, \\ \int \psi(x,t)dx = 1, \forall t \in D.$$

For each fixed $t \in D$ we define an *admissible averaging kernel* to be the function

$$\psi^\epsilon(x,t) \equiv \frac{1}{\epsilon}\psi(\frac{x}{\epsilon},t). \tag{11}$$

The kernel is *symmetric* if $\int_{x<0} \psi(x,t)dx = \frac{1}{2}$.

Let v be a bounded, measurable function defined on D. For $(x_0,t) \in D$ denote

$$T(\psi)v(x_0,t) = \lim_{\epsilon\to 0} \int \psi^\epsilon(x-x_0,t)v(x,t)dx. \tag{12}$$

For a fixed t we shall say that the *mean value with respect to x* of the function $v(x,t)$ exists at the point (x_0,t) if the limit in (12) is finite. A *symmetric mean with respect to x, i. e.*, the mean corresponding to a symmetric kernel, will be denoted by $S(\psi)v(x_0,t)$.

Theorem 2.1. *Let v be a bounded, measurable function, defined in the neighborhood of (x_0,t). Then the mean value with respect to x, $T(\psi)v(x_0,t)$, exists for any admissible averaging kernel ψ, and*

$$T(\psi)v(x_0,t) = v(x_0-,t)\int_{x<0} \psi(x,t)dx \\ + v(x_0+,t)\int_{x>0}\psi(x,t)dx. \tag{13}$$

This is a direct consequence of Theorem 10.2 in [17].

Corollary 2.1. *[17] The symmetric mean is equal to*

$$S(\psi)v(x_0,t) = \frac{1}{2}\left[v(x_0-,t) + v(x_0+,t)\right], \tag{14}$$

and therefore the symmetric mean does not depend on the choice of the kernel.

To define the product $\int u_x a(x)u\phi$ we first regularize u_x. Let D be a bounded subset of the (x,t)-plane and let u be a bounded and measurable function on D. Denote by H_2 the Heaviside function

$$H_2(x,t) = \begin{cases} 1 \text{ if} & x \geq x_*, \\ 0 \text{ if} & x < x_*. \end{cases} \tag{15}$$

Define

$$u^L(x,t) = \begin{cases} u(x,t) & \text{if} \quad x < x_* \\ u(x_*-,t) & \text{if} \quad x \geq x_*, \end{cases} \tag{16}$$

and

$$u^R(x,t) = \begin{cases} u(x_*+,t) & \text{if} \quad x \leq x_* \\ u(x,t) & \text{if} \quad x > x_*, \end{cases} \tag{17}$$

where by $u(x_*\pm,t)$ we denoted the limit of u from the left (right, respectively), as $x \to x_*\pm$. We write

$$u = u(I-H_2) + uH_2 = u^L(I-H_2) + u^R H_2. \tag{18}$$

Then the derivative of u in the sense of distributions can be written as

$$u_x = u_x^L(I-H_2) - u^L(H_2)_x + u_x^R H_2 + u^R(H_2)_x \\ = (u^R - u^L)(H_2)_x + u_x^L(I-H_2) + u_x^R H_2.$$

We regularize u_x by using an admissible averaging kernel ψ^ϵ to approximate the Dirac delta function $(H_2)_x$

$$u_x^{\psi^\epsilon} = (u^R - u^L)\psi^\epsilon(x-x_*,t) + u_x^L(I-H_2) + u_x^R H_2. \tag{19}$$

We define the product

$$\langle u_x a(x) u\phi\rangle_\psi = \int u_x a(x)u\phi \equiv \lim_{\epsilon\to 0}\int\int_{t\geq 0} u_x^{\psi^\epsilon}(au)\phi. \tag{20}$$

More precisely,

$$\langle u_x a(x) u\phi\rangle_\psi = (u^R - u^L)\int_{t\geq 0} T(\psi)\,(au\phi)(x_*,t)dt \\ + \int\int u_x^L(au\phi)(I-H_2) + u_x^R(au\phi)H_2\,dx\,dt. \tag{21}$$

Notice that if the kernel is symmetric, the product is independent of the choice of the kernel.

We say that a bounded, measurable function u satisfies the *ψ-weak form* of equation (9) if for all $\phi \in C_0^\infty$

$$\int\int_{t\geq 0}\left(u\phi_t + (a(x)u^2)\phi_x\right)dx\,dt + \langle u_x a(x)u\rangle_\psi = 0. \tag{22}$$

Theorem 2.2. *The solution u of the ψ-weak form (22) satisfies the following jump condition across the discontinuity $x = x_*$*

$$[au^2] - [u]\overline{au}^\psi = 0, \tag{23}$$

where $\overline{au}^\psi = T(\psi)au(x_*,t)$. If ψ is symmetric $\overline{au}^\psi$ is independent of the choice of the kernel and it will be denoted by $\overline{au}$ where $\overline{au} = \frac{1}{2}\left((au)(x_*-,t) + (au)(x_*+,t)\right)$.

Proof. Let u be a solution of the ψ-weak form (22) and let D be again a small neighborhood of a fixed point (x_*,t). Then

$$-\int_D u\phi_t + (au^2)\phi_x = \langle u_x a(x)u\rangle_\psi, \quad \forall\phi \in C_0^\infty(D).$$

Since the left hand-side involves only conservative products, standard manipulations give

$$\int_{D_1}\left(u_t + (au^2)_x\right)\phi + \int_{D_2}\left(u_t + (au^2)_x\right)\phi \\ + \int_{\{x=x_*\}\cap D}[au^2]\phi dt = \langle u_x a(x)u\rangle_\psi$$

where $[au^2]$ is the jump of au^2 across the discontinuity $x = x_*$ and D_1 and D_2 are the subsets of D lying on either side of $x = x_*$. To deal with the right hand-side we use (20) and (13) to obtain

$$\int_{D_1}\left(u_t + (au^2)_x\right)\phi + \int_{D_2}\left(u_t + (au^2)_x\right)\phi \\ + \int_{\{x=x_*\}}[au^2]\phi dt = \int_{\{x=x_*\}}[u]T(\psi)\,(au\phi)(x_*,t)dt \\ + \int_{D_1} u_x(a(x)u)\phi + \int_{D_2} u_x(a(x)u)\phi. \tag{24}$$

Since $u_t + (au^2)_x = auu_x$ holds in the interior of each subdomain the combined integrals over D_1 and the combined integrals over D_2 vanish. Using the fact that ϕ is continuous, the remaining terms read

$$\int_{\{x=x_*\}} \left([au^2] - [u]T(\psi)(au)\right) \phi dt = 0, \quad \forall \phi \in C_0^\infty,$$

and we recover the jump condition across the discontinuity $x = x_*$: $[au^2] - [u]\overline{au}^\psi = 0$.

Remark 2.1. If ψ is symmetric, we would have recovered the same jump condition if we had regularized the term $(a(x)u)_x$ in the original equation. This is because $\bar{f}[g] = [fg] - [f]\bar{g}$ where $\bar{f}$ is the symmetric average (arithmetic mean) of f. More precisely, if $f(x,u)$ and $g(x,u)$ are two functions, possibly discontinuous with a jump discontinuity at $x = x_*$, then the above approach implies that the jump of the product fg_x is equal to the jump of $(fg)_x - f_x g$.

Corollary 2.2. *The jump condition that is satisfied by the solution of the ψ-weak form of (9) in the case when ψ is symmetric, and with the coefficient a given by (7) reads*

$$u_R = \frac{a_L u_0}{a_R}. \tag{25}$$

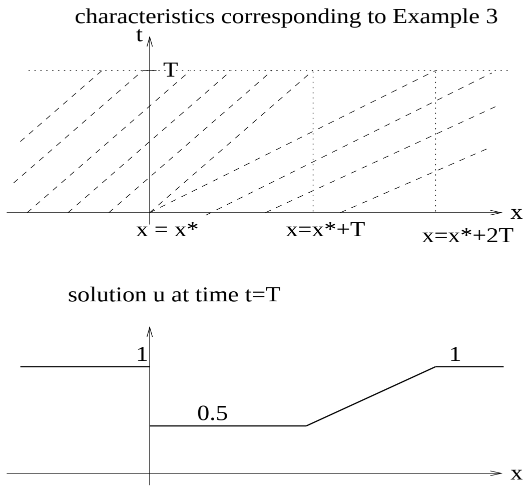

Fig. 3. Solution corresponding to Example 3

We now complete the ψ-weak solution of equation (9) in the case when ψ is symmetric and assuming, for example, $u_0 = 1, a_L = 1, a_R = 2$. The slopes of the characteristics are $\frac{dx}{dt} = au$. The solution is equal to $u = 1$ on the left of $x = x_*$, then it jumps from 1 to 0.5 on the right of $x = x_*$ and above the characteristic $x - x_* = t$. Then there is a rarefaction wave in the region bounded by the characteristics $x - x_* = t$ and $x - x_* = 2t$, and finally $u = 1$ on the right of $x - x_* = 2t$. See Figure 3. Notice that in this case the characteristics are smooth, $\dot{x} = 1$, across the jump discontinuity $x = x_*$.

3 Numerical Simulations

We used the Richtmyer two-step Lax-Wendroff method as presented in [13] and the classical Lax-Friedrichs method to calculate the solution from Example 3. The two-step Lax-Wendroff method recovers the ψ-weak solution, presented in Theorem 2.2, corresponding to a symmetric kernel ψ. In Figure 4 we show the exact solution in dashed line, and the computed solution in solid line. The numerical simulation in Figure 4 was obtained with $dx = 0.01$, on the computational domain $0 \leq x \leq 2$, with the initial condition $u_0 = 1$, and $a_L = 1$ and $a_R = 2$. Notice that we recover the right state $u_R = 0.5$. The same right state is obtained if the coefficient a is smoothed out. In that case the jump discontinuity at $x = x_*$ is spread over several mesh blocks. The reasons for why

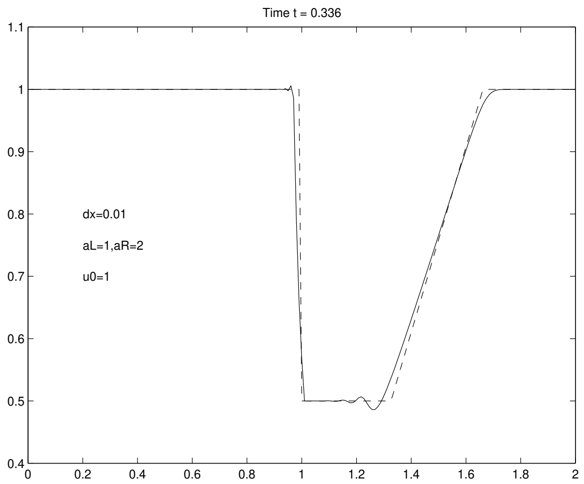

Fig. 4. Solution corresponding to Example 3

this numerical method produces the solution corresponding to the ψ-weak form with a symmetric ψ are under investigation by the author. We also note that the classical Lax-Friedrichs method produced a different solution; the right state at the jump discontinuity located at x_* is $u_R = 0.55$. A solution which is different from the solution obtained using the Lax-Wendroff method could have perhaps been expected since it is well known that this method does not behave well around discontinuous solution for equations not in conservation form.

4 Analysis of the Model Equations

In this section we study the model equations (1) and (2). We are assuming that the pressure coefficients are discontinuous at $x = x_*$ and study the behavior of the state variables A and m across the locus $x = x_*$. It can be easily seen (Therem 4.1 below) that the weak form of the mass conservation equation implies that m has to be continuous across $x = x_*$. So m behaves like the solution in Example 1 from Section 2. Assuming that A is also continuous, one can write the weak form of the second equation in a standard way and show that this assumption is in contradiction with the fact that the coefficients of p are discontinuous. So A behaves essentially like the solution in Example 3 from Section 2. Since A is not continuous at $x = x_*$ we use the approach presented in Section 2 and derive the ψ-weak form of the equations by regularizing the Dirac delta function term using an admissible averaging kernel. We derive the ψ-jump condition across $x = x_*$ satisfied by the weak solutions of the ψ-weak form. In the next section we show that the Lax-Wendroff method applied to the system (1) and (2) recovers the solution which satisfies the derived ψ-jump condition with a symmetric averaging kernel ψ.

Theorem 4.1. *Let x_* be a point of discontinuity of the pressure coefficients. Then A is discontinuous at x_* and m is continuous there.*

Proof. The first equation is linear and the standard weak form of the equations leads to the Rankine-Hugoniot condition

$$-s\,[A] + [m] = 0.$$

Since $s = 0$ we obtain $[m] = 0$.

Assume that A is continuous. Using the same approach as in Example 3 we can write equation (2) as

$$\int\int_D m\phi_t + \alpha\frac{m^2}{A}\phi_x + Ap(x,A)\phi_x = \int\int_D A_x p(x,A)\phi$$

for all $\phi \in C_0^\infty(D)$. Let D_1 and D_2 be the subsets of the set D lying on either side of the locus $x = x_*$. Since A is assumed to be continuous, we can write all the integrals, including the one of the right hand-side, as the sum of two integrals, one over D_1 and one over D_2. The rest proceeds in the usual way. Denote by $\mathbf{n_1}$ the unit normal to the boundary of D_1, and by $\mathbf{n_2}$ the unit normal to D_2, then integration by parts one more time leads

$$\begin{aligned}
&\int_{\partial D_1}\mathbf{F}\cdot\mathbf{n_1} + \int\int_{D_1}\left(m_t + \left(\alpha\frac{m^2}{A} + Ap(x,A)\right)_x\right)\phi\\
&+\int_{\partial D_2}\mathbf{F}\cdot\mathbf{n_2} + \int\int_{D_2}\left(m_t + \left(\alpha\frac{m^2}{A} + Ap(x,A)\right)_x\right)\phi\\
&= \int\int_{D_1} A_x p(x,A)\phi + \int\int_{D_2} A_x p(x,A)\phi, \quad \forall\phi\in C_0^\infty(D),
\end{aligned}$$

where

$$\mathbf{F} = \left(m, \alpha\frac{m^2}{A} + Ap(x,A)\right)^T.$$

Since $m_t + \left(\alpha\frac{m^2}{A} + Ap(x,A)\right)_x = A_x p(x,A)$ holds in the interior of D_1 and D_2, all that is left in the above equation is the jump in the vector field $\mathbf{F}$ across the locus $x = x_*$

$$-s\,[m] + \left[\alpha\frac{m^2}{A}\right] + [Ap(x,A)] = 0.$$

Since $s = 0$ and A and m are continuous, this equation becomes

$$p_R(x,A) - p_L(x,A) = 0,$$

where $p_L(x,A)$ and $p_R(x,A)$ denote the limits of the transmural pressure from the left and from the right, respectively, $p_L(x,A) = \lim_{x\to x_*-} p(x,A)$, $p_R(x,A) = \lim_{x\to x_*+} p(x,A)$. This is in contradiction with the assumption that p has discontinuous coefficients. Thus, A cannot be continuous across $x = x_*$. This concludes the proof.

We use the same approach as presented in Section 2 and derive the ψ-weak form of the equations. Let H_2, A^L, A^R be defined as in Example 3 by using (15), (16) and (17). Let ψ^ϵ be an admissible averaging kernel defined by (11). We define A_x^ϵ to be

$$A_x^{\psi^\epsilon} = (A^R - A^L)\psi^\epsilon(x - x_*, t) + A_x^L(I - H_2) + A_x^R H_2. \tag{26}$$

We say that a bounded, measurable function (A, m) satisfies the *ψ-weak form* of the equations (1) and (2) if for all $\phi\in C_0^\infty$ the following equations are satisfied

$$\begin{aligned}
&\int_{t\geq 0} A\phi_t + m\phi_x = 0\\
&\int_{t\geq 0} m\phi_t + \left(\alpha\tfrac{m^2}{A} + \tfrac{1}{\rho}Ap(x,A)\right)\phi_x + f(m,A)\phi\\
&= -\tfrac{1}{\rho}\left\langle A_x p(x,A)\phi\right\rangle_\psi,
\end{aligned} \tag{27}$$

where

$$\begin{aligned}
\left\langle A_x p(x,A)\phi\right\rangle_\psi &= \lim_{\epsilon\to 0}\int_{t\geq 0} A_x^{\psi^\epsilon} p(x,A)\phi =\\
&\int_{t\geq 0}[A]T(\psi)\,(p\phi)(x_*,t)dt\\
&+\int\int A_x^L(p\phi)(I - H_2) + A_x^R(p\phi)H_2\,dx\,dt.
\end{aligned}$$

Theorem 4.2. *The solution of the ψ-weak form (27) satisfies the following jump conditions across the locus where the pressure coefficients are discontinuous*

$$-s\,[A] + [m] = 0 \tag{28}$$

$$-s\,[m] + \left[\alpha\tfrac{m^2}{A}\right] + \tfrac{1}{\rho}\left([A\,p(x,A)] - [A]\,\overline{p(x,A)}^\psi\right) = 0 \tag{29}$$

where $\overline{p(x,A)}^\psi = T(\psi)p(x,A)$. When ψ is symmetric, $\overline{p(x,A)}^\psi$ does not depend on the choice of the kernel and it is equal to the arithmetic mean $\overline{p} = \frac{1}{2}(p_L + p_R)$ between the values of the pressure on either side of the discontinuity.

The proof follows the same steps as the proof of Theorem 2.2.

Notice that when ψ is symmetric, the second condition is the same as

$$-s\,[m] + \left[\alpha\frac{m^2}{A}\right] + \frac{1}{\rho}\overline{A}\,[p] = 0.$$

Since in our problem $s = 0$ and m is continuous, the second jump condition implies that across $x = x_*$

$$-\alpha m^2\left[\frac{1}{A}\right] + \frac{1}{\rho}\overline{A}\,[p] = 0. \tag{30}$$

5 Example: Abdominal Aortic Aneurysm

Aneurysm is characterized by the formation of sac-like protrusions of weakened sections of blood vessels that can rupture and be fatal. Endoluminal treatment of aortic aneurysm entails inserting a catheter (a hollow tube) into an artery and directing it to the site of the aneurysm. Placed in the catheter is a spring-like device called a stent, see Figure 5, which serves to hold open the weakened artery and to exclude the aneurysm from circulation. Near the anchoring sites of the stent, the stent and

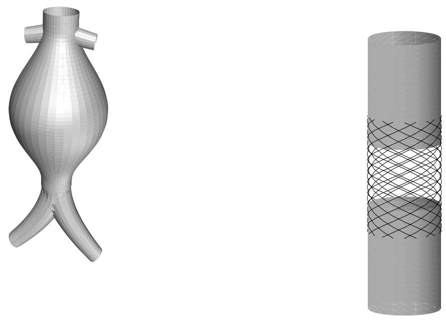

Fig. 5. A sketch of abdominal aneurysm (left) and a sketch of a stent inserted in the abdominal aorta(right)

the aorta overlap, whereas inside the aneurysmal cavity, the stent is not supported by the walls of the aorta, at least in the early stages after the repair. In Figure 5 on the right, the flow channel in this region consists of the stent only (the aneurysmal pouch is not shown). Usually within six to eight weeks the endothelial cells completely cover the stented part of the channel. After six months, if there is no endoleak, the aneurysmal pouch thromboses and provides support to the walls of the stent.

To simulate, for example, the blood flow in the early stages after the repair, the parameter G_0 has the smallest values in the region where the stent is not supported by the aorta. We will consider three overlapping stents of equal length, which is practiced by several cardiologists to make the pores in the prosthesis smaller. Based on the measurements obtained by Ravi Chandar [5] the Young modulus of the stent is ten times smaller than the Young modulus of the native aorta. Using the data obtained in [15] we assume that $G_0 = 4 \times 10^4 N/m^2$ for the abdominal aorta, G_0 is three times the Young modulus corresponding to a single stent, which is $4 \times 10^3 N/m^2$ [5], and G_0 is the sum of the two coefficients in the region where the two overlap [3,7]. We assume $\beta = 2$. We focus on the abdominal aorta in the region between renal and iliac arteries. We assume that this length is typically 0.1 m $(0 \leq x \leq 0.1)$ and that a 4 cm triple stent prosthesis is placed in the region $0.3 \leq x \leq 0.7$. Furthermore, we assume that, at the anchoring sites, the prosthesis is placed 1 cm deep in the nonaneurysmal part of the aorta. The data used in the simulation are: blood density $\rho = 1050 kg/m^3$, viscosity $\nu = 3.2 \times 10^{-6} m^2/s$ and unstressed radius of the abdominal aorta $R_0 = 0.0082m$.

We ran the simulations with pulsatile flow boundary data on the left, and with "transparent boundary condition" on the right end of the computational domain. Figure 6 shows the cross-sectional area at the peak of the systol in one cardiac cycle.

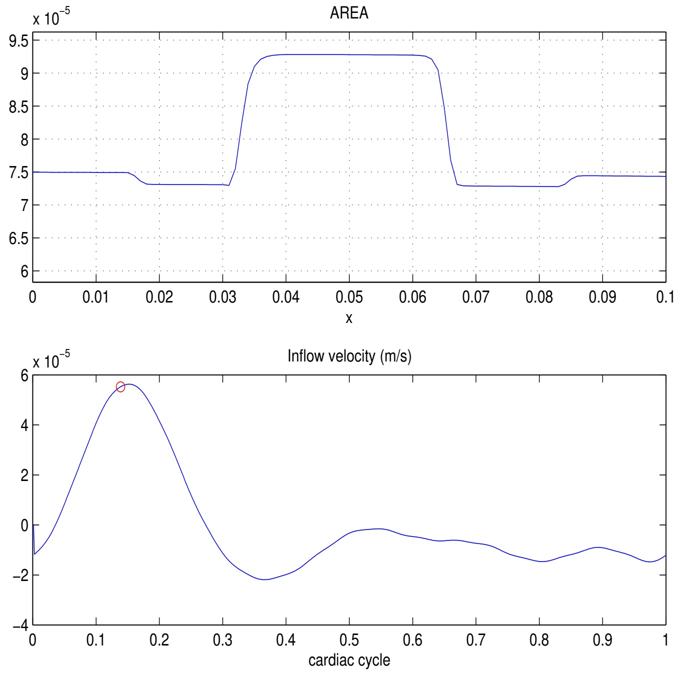

Fig. 6. Cross-sectional area at the peak of the systol

We used equation (30) to estimate the jump in the cross-sectional area of the channel at the point where the prosthesis stops being supported by the aorta. This happens at $x = 0.033$ in Figure 6. The cross-sectional area on the left is obtained from the numerical simulation and equals $A_L = 7.296 \times 10^{-5}$ at $x = 0.03$. Using (30) we calculated the state on the right of the discontinuity and obtained $A_R = 9.28431 \times 10^{-5}$ when ψ is symmetric. We compared this value of A_R with the value of A_R at $x = 0.04$ obtained in the numerical simulation using the two-step Lax-Wendroff method which is $A_R = 9.2807 \times 10^{-5}$. See Figure 6. The two are in excellent agreement.

6 Conclusions

In this paper we presented a preliminary analysis leading to the equations (28) and (29) which can be used to study wall deformations induced by the rapidly changing wall properties. In the case of abdominal aortic aneurysm equations (28) and (29) can be used in designing optimal strategies for the treatment of abdominal aneurysm using multiple overlapping stents since the equations provide information regarding transmural pressure and wall deformation at the anchoring sites of the stent. High transmural pressure and high deformations can be directly linked to various short and long term complications reported after endovascular repair of aortic aneurysm [16].

References

1. M. Back, G. Kopchok, m. Mueller, D. Cavaye, C. Donayre, and R. White. Changes in arterial wall compliance after endovascular stenting. *Journal of Vascular Surgery*, 905–911, May 1994.
2. A. C. L. Barnard, W. A. Hunt, W. P. Timlake, and E. Varley. A theory of fluid flow in compliant tubes. *Biophys. J.*, 6:717–724, 1966.
3. S. Čanić, and D. Mirković. A Hyperbolic System of Conservation Laws in Modeling Endovascular Treatement of Abdominal Aneurysm. *Proceedings of the 8th International Conference on Hyperbolic Problems, HYP2000*, to appear.
4. S. Čanić. Blood flow modeled by a hyperbolic system of conservation laws: a proof that shocks do not form in a healthy abdominal aorta. *In preparation.*
5. R. Wang, and K. Ravi-Chandar. Mechanical Response of a Metallic Aortic Stent *EMRL Report Number: 01-01 Center for Mechanics of Solids, Structures and Materials The University of Texas at Austin*
6. C. Dafermos. Hyperbolic Conservation Laws in Continuum Physics. *A Series of Comprehensive Studies in Mathematics* Volume 325 Springer New York (2000).
7. J. F. Dyet, W. G. Watts, D. E. Ettles, and A. A. Nicholson. Mechanical properties of metallic stents: How do these properties influence the choice of stent for specific lesions? *Cardiovsc. Interv. Radiology*, 23:47–54, 2000.
8. L. Formaggia, F. Nobile, and A. Quarteroni. A one dimensional model for blood flow: application to vascular prosthesis. *Proceedings of the MSCOM2000 conference*, to appear.
9. L. Formaggia, J.-F. Garbeau, F. Nobile, and A. Quarteroni. On the coupling of 3D and 1D Navier-Stokes equations for flow problems in compliant vessels. *Ècole Polytechnique Fèdèrale de Lausanne* Preprint.
10. L. Gosse, and F. James. Numerical approximations of one-dimensional linear conservation equations with discontinuous coefficients. *Math. Comp.* 69:987–1015 (2000).
11. J. Keener, and J. Sneyd. Mathematical Physiology. *Interdisciplinary Applied Mathematics* Volume 8 (1998) Springer New York.
12. A. Achari and Z. Krajcer. A novel method for endoluminal treatment of abdominal aortic aneurysms. *Cardiovascular Interventions, Texas Heart Institute Journal*, 25:44–48, 1998.
13. R. J. LeVeque. *Numerical Methods for Conservation Laws.* Birkhäuser, Boston, 1992.
14. C. Peskin. Partial Differential Equations in Biology. *Courant Institute of Mathematical Sciences Lecture Notes* New York (1975).
15. S. T. R. MacSweeney, G. Young, R. M. Greenhalgh, and J. T. Powel. Mechanical properties of the aneurysmal aorta. *Br. J. Surg.*, 79:1281–1284, 1992.
16. T. Umscheid and W. J. Stelter. Time-related alterations in shape, position, and structure of self-expanding, modular aortic stent-grafts. *J. Endovasc. Surg.*, 6:17–32, 1999.
17. A. I. Vol'pert. The spaces BV and quasilinear equations. *Mat. Sbornik* Tom 73(115) No.2 (1967).